ORIGINAL ARTICLE

A novel biological approach on extracellular synthesis and characterization of semiconductor zinc sulfide nanoparticles

Chelladurai Malarkodi · Gurusamy Annadurai

Abstract The expansion of reliable and eco-friendly process for synthesis of semiconductor nanoparticle is an important step in the emerging field of biomedical nanotechnology. In this communication, the zinc sulfide nanoparticles were biologically synthesized by using *Serratia nematodiphila* which was isolated from chemical company effluent. The surface plasmon resonance centered at 390 nm on the UV spectrum indicates the presence of zinc sulfide nanoparticles in the reaction mixture (*S. nematodiphila* and zinc sulfate); EDAX analysis also confirmed the presence of zinc sulfide nanoparticles. Scanning electron microscope image showed that the synthesized zinc sulfide nanoparticles were spherical in nature and nanoparticles of about 80 nm in size were obtained from transmission electron microscope images. The peaks in the XRD spectrum corresponding to (111), (220) and (311) show that the zinc sulfide nanoparticles are crystalline in nature. Fourier transforms infrared spectroscopy shows the functional groups of the nanoparticle in the range of 4,000–400 cm^{-1}. Further, the antibacterial activity of zinc sulfide nanoparticles was examined against *Bacillus subtilis* and *Klebsiella planticola*. The maximum zone of inhibition occurred at 200 μl of silver nanoparticles. Due to potent antimicrobial and intrinsic properties of zinc sulfide, it is actively used for biomedical and food packaging applications.

Introduction

Nanotechnology deals with the creation of materials less than 100 nm in dimension and has taken precedence in several fields including biotechnology, biomedical sciences, and material sciences and engineering. The development of semiconductor nanoparticles by using bio-route is an interesting progress in the modern research of nanotechnology. Considerable enthusiasm is now emerging from the current literature about the multidisciplinary field of nanobiotechnology within biological systems (Penn et al. 2003; Riddin et al. 2006). Recently, the synthesis of chalcogenides of different groups has involved considerable awareness due to their important nonlinear (Brus 1991) luminescent properties, quantum size effects and other important physical and chemical properties (Murray et al. 1995; Qiao et al. 2000). ZnS is a semiconductor nanomaterial possessing a lot of interesting physical properties and potentially used in mesoscopic electronic (Stanley 1975; Ni et al. 2004) biolabeling (Elghanian et al. 1997) and photocatalysis (Hoffmann et al. 1995). The semiconductor nanocrystals are used to eradicate environmental hazardous materials such as heavy metals and dyes through photocatalytic degradation of water contaminants (Mills and Hunte 1997; Kho et al. 2000). The budding process of the zinc sulfide nanocrystals may be well described by power laws (Zhang et al. 2002; Khiewa et al. 2005). *Clostridium thermoaceticum* and *Klebsiella aerigenes* are used to form the CdS nanoparticles (Mandal et al. 2006). The bacteria grow aerobically and anaerobically due to dark and light conditions and have tolerance to

C. Malarkodi · G. Annadurai (✉)
Environmental Nanotechnology Division, Sri Paramakalyani Centre for Environmental Sciences, Manonmaniam Sundaranar University, Alwarkurichi 627412, Tamil Nadu, India
e-mail: gannadurai@hotmail.com

C. Malarkodi
e-mail: malarebt@gmail.com

heavy metals (Giotta et al. 2006; Bai and Zhang 2006). The microorganism has endogenous aptitude to regulate the synthesis of inorganic materials such as amorphous silica (diatoms), magnetotatic bacteria, gypsum and calcium carbonate layers (S-layer bacteria) and raw materials such as calcite into functional superstructures (Mandal et al. 2006). The intracellular synthesis of CdS quantum dots in *Schizosaccharomyes pombe* yeast cells demonstrates idle diode characteristics. The biogenic CdS nanoparticle has been used in the fabrication of a heterojunction with poly (p-phenylenevinylene) (Kowshik et al. 2002; Baia et al. 2009). The heavy metal ion against microorganism has been exploited for biological metal healing in the reduction of metal ion and formation of metal sulfide nanoparticles. The chemical and physical procedures could be used for the synthesis of semiconductor nanoparticle; however, these methods are fraught with many problems including use of toxic solvents, generation of hazardous by-products and high energy consumption. Accordingly, there is an essential need to develop environmentally benign procedures for synthesis of nanoparticles (Riddin et al. 2006). The biological synthesis of nanoparticle has been currently explored through bacteria (Joerger et al. 2000), yeast (Kowshik et al. 2003), fungi (Mandal et al. 2006), plant biomass (Armendariz et al. 2004) and live plants (Sharma et al. 2007; Longoria et al. 2011). There are several studies on microorganism or enzyme performing the transportation for the bioreduction of metals, but the mechanism for this process remains elusive. Recently, it was verified that the hydrogenase enzymes in a sulfidogenic bioreactor containing a mixed group of sulfate-reducing bacteria were able to reduce Rh (III) (Ngwenya and Whiteley 2006) and Pt (IV) (Rashamuse and Whiteley 2007) to their particular metallic form under a hydrogen atmosphere. In bioremediation applications, sulfate-reducing bacteria removed the metals from the water stream and precipitated the hydrogen sulfide during their respiration process (Webb et al. 1998; Khan et al. 2004; Håkansson and Mattiasson 2002). *Serratia nematodiphila* is a red-pigmented, nonspore-forming fluorescent strain associated with the entamopathogenic nematode (Zhang et al. 2008; Zhang et al. 2009). This work demonstrated the extracellular synthesis of stable zinc sulfide nanoparticle using the bacteria *S. nematodiphila*.

Materials and methods

Isolation and identification of microorganism

The sulfur-reducing bacteria were isolated from a chemical company effluent and the samples were collected from Vellore. The collection of samples was serially diluted and inoculated in a sulfur-reducing medium (SRB) for isolation of sulfur-reducing bacteria. Further, the sulfur-reducing bacteria were grown in SRB medium containing (g/l) 1.5 g of sodium sulfate, 0.5 g of K_2HPO_4, 3.5 g of sodium lactate, 1.0 g of beef extract, 2.0 g of peptone, 0.1 g of calcium chloride, 0.392 g of ferrous ammonium sulfate, 2.0 g of magnesium sulfate and 0.1 g of sodium ascorbate (Jones 1971). The organism was incubated at 30–35 °C. The isolates were morphologically and microbiologically characterized as *S. nematodiphila*. The isolated culture was identified as *S. nematodiphila* (CAA) from MTCC and maintained by a subculture process for synthesis of zinc sulfide nanoparticles.

Extracellular synthesis of zinc sulfide nanoparticle

The strain *S. nematodiphila* (CAA) was grown in 100 ml of nutrient broth and incubated at 35 °C for 24 h. The overnight culture broth was centrifuged at 6,000 rpm for 10 min. The cell-free supernatants were collected and 1 mM of zinc sulfate was added and mixed, and the solution was incubated at 35 °C for 24 h. The spectrum of the sample was measured by UV–visible spectrophotometer.

Characterization of nanoparticle

The synthesized zinc sulfide nanoparticle was air dried and used for analysis. The UV–visible spectrum was recorded with Perkin-Elmer spectrophotometer, with wavelength ranging from 300 to 700 nm. The morphology and particle size were determined by transmission electron microscopy (TEM) operating on Hitachi Model H-800 using an accelerating voltage of 200 kV. Scanning electron microscopy (SEM) was performed with a HITACHI Model S-3000H by focusing on nanoparticles. To check phase formation and purity, powder XRD patterns were recorded using an X-ray diffractometer (X'per PRO model) using CuKα radiation, at 40 keV in the 2θ range of 10–80. The zinc sulfide nanoparticles were subjected to Fourier transform infrared spectroscopy (FTIR) studies which were carried out in a MAKE-BRUKER Optik GmbH MODEL No-TENSOR 27. The samples were dried and ground with KBr. Infrared spectra were measured at the wavelength range from 4,000 to 400 cm^{-1}.

Antibacterial activity of zinc sulfide nanoparticles

The end products of the zinc sulfide nanoparticles were used to study the antibacterial activity against Gram-positive bacteria *Bacillus subtilis* (MTCC 3053) and the Gram-negative bacteria *K. planticola* (MTCC 2277) with disc diffusion method by culturing the microorganism in Muller Hinton agar. The sterile discs were dipped into the

different concentrations of zinc sulfide nanoparticles, 50, 100 and 200 µl, respectively. After a few minutes of air drying, the dried discs were gently placed into the agar and incubated for 24 h. After 24 h of incubation at 35 °C, the zone of inhibition of nanoparticles against bacteria was observed. The sterile disc without nanoparticles was noted as the control. Three replicates of experiments were carried out.

Results and discussion

In this study, the bacterial strain used for the synthesis of zinc sulfide nanoparticles was isolated from a chemical company wastewater. The isolate strain CAA was morphologically and biochemically identified as *S. nematodiphila* that produces a red pigment. *S. nematodiphila* (CAA) was a Gram-positive, rod-shaped and nonmotile bacteria identified and maintained at Microbial Type Culture Collection and Gene bank (MTCC), Chandigarh. *S. nematodiphila* belongs to the family Enterobacteriaceae of the class Gammaproteobacteria. Some types of the *Serratia* contain clinical importance (Grimont et al. 1988) and the other group of genus produce pigments identified as prodigiosin (Hearn et al. 1970; Zhang et al. 2009).

The biosynthetic route using *S. nematodiphila* (CAA) has been developed for the zinc sulfide nanoparticle production and was used in this work. During the visual observation, the color of the culture supernatant incubated with zinc sulfate (inset Fig. 1a, b) changed from yellow to whitish yellow. Figure 1a shows that no color change could be observed in the culture supernatant without zinc sulfate in the 24-h bacterial biomass. The appearance of a whitish yellow color in the zinc sulfate-treated flask suggested the formation of zinc sulfide nanoparticles (inset Fig. 1b).
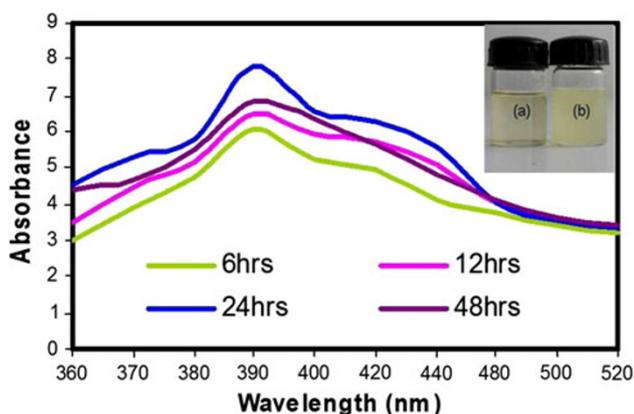
The UV–vis spectra (Fig. 1) were recorded from the *S. nematodiphila* (CAA).

Biosynthesis of zinc sulfide nanoparticle using *S. nematodiphila* (CAA) was monitored in the UV–Vis spectrophotometer. The broad peak was located between 380 to 400 nm and the strong absorbance centered at 390 nm. Figure 1 shows the zinc sulfide nanoparticles formation and maximum production at 24 h of incubation. The broadening of the peak at 390 nm due to the quantum confinement effect (Zhao et al. 2006) occurs during the size reduction of nanoparticles by *S. nematodiphila* (CAA). After 48 h of incubation, the rate of nanoparticle formation was reduced.

The X-ray diffraction pattern in Fig. 2 corresponds to that of zinc sulfide nanoparticle powder. The three intense peaks in the whole spectrum of 2θ values range from 20 to 80°. The diffractions spectrum of nanocrystals has three similar characteristic peaks, 28.61, 48.12 and 58.02°, can be indexed to the (111), (220) and (311) planes of the face-centered cubic, respectively, by comparison with the data from JPCDS file no 5-0566, which indicates the biological synthesis of zinc sulfide nanoparticle by *S. nematodiphila*. The full widths at half maximum (FWHM) values measured for (220) planes of reflection were used with the Debye–Scherer equation to calculate the size of the nanoparticle.

$$D = K\lambda/\beta(\cos\theta).$$

The equation uses the suggestion peak width at Bragg diffraction angle θ, where K is a Blank's constant, λ is the source wavelength (1.54), and β is the width of the XRD peak at half maximum height. The calculated average particle size of the zinc sulfide nanocrystals was found to be 6.77 nm.
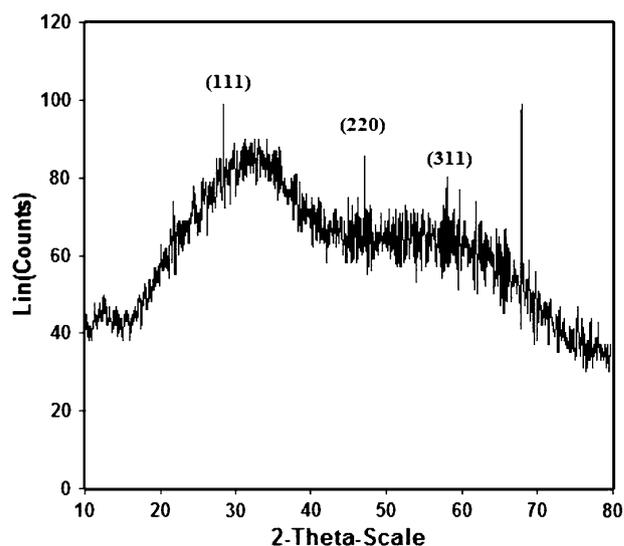

Fig. 1 UV–Vis absorption spectrum of zinc sulfide nanoparticle. *Inset* **a** shows test tube containing the culture supernatant of *S. nematodiphila*, **b** *S. nematodiphila* biomass with zinc sulfate

Fig. 2 XRD pattern of zinc sulfide nanoparticle

The morphology of zinc sulfide nanoparticles was characterized by scanning electron microscope, which was confirmed to be of zinc by EDX. *S. nematodiphila* (CAA) treated with the zinc sulfate nanoparticle is well dispersed. At different magnification like 20,000×, the particles were approximately in the range of 1–5 μm (scale bar). Zinc sulfide nanoparticles that formed were spherical in shape (Fig. 3a, b). Similar result of the shape of the zinc sulfide nanoparticles was reported by using the chemical synthesis method (Subhendu et al. 2007). EDX analysis (Fig. 4) shows strong peak in the zinc sulfide, confirming the presence of semiconductor zinc sulfide nanocrystallites at atomic ratio of 47:18, which is characteristic for the absorption of zinc. The undesigned peaks at C, O, S is held to have the absorption of excessive contamination on the surface of the nanoparticle. Similarly, a strong peak is observed in Zn and the atomic ratio of zinc sulfide, calculated from the quantified action, peaked at 1:1 (Khiewa et al. 2005).

The TEM technique is used to visualize the shape and size of the zinc sulfide nanoparticles, formed in different sizes, ranging from polydispersed small spherical to large spherical shapes. Figure 5(a) shows that zinc sulfide nanocrystals polydisperse and are mostly spherical in shape, well distributed with aggregation in solution in the size range of 80 nm. Some of the particles are agglomerated. The reason for the increase in the particle size as the bacteria grow from the exponential phase to the stationary phase is probably due to "nucleation effect," where small particles agglomerate to form larger particles (Bai and Zhang 2006). It is believed that the same reason applies for the nanoparticle agglomeration. The long-term stability of the zinc sulfide nanoparticle in the solution may be due to the lack of stabilizing agents is proteins. The inset in Fig. 5b shows that the selected area electron diffraction (SAED) pattern indicates three sharp rings of zinc sulfide nanoparticle. The sharp rings revealed the polycrystalline nature of the nanoparticle. The diffraction rings can be indexed to (111), (220) and (311) planes of the cubic zinc sulfide phase. Similar three concentric rings are observed in the zinc sulfide nanoparticle, indicating that the particles are crystalline in nature (Ni et al. 2004).

Figure 6 shows the FTIR spectrum recorded from the freeze-dried powder of zinc sulfide nanoparticles, formed after 24 h of incubation with the bacteria. The amino acid residues and peptides of proteins present the well-known signatures in the infrared region of the electromagnetic spectrum. The broad bands seen at 3,434 cm^{-1} are assigned to the C–H stretching vibrations due to phenol amide linkages of the protein, and 1,659 cm^{-1} bands reveal the C=O stretching vibrations of alkynes or amides and are frequently diagnostic of unsaturation, while their weak bending vibrations correspond to 2,952 and 1,538 cm^{-1}. The small peaks observed at 1,404 cm^{-1} correspond to the O–H bending vibrations of aromatic or carboxylic groups. The band 1,236 and 1,060 cm^{-1} can be assigned to the C–N vibrations in the amine or aliphatic groups, respectively. The peak at 592 cm^{-1} was assigned to the alkyl

Fig. 3 SEM micrograph of zinc sulfide nanoparticles formed after reaction of culture supernatant with 1 mM zinc sulfate for 24 h
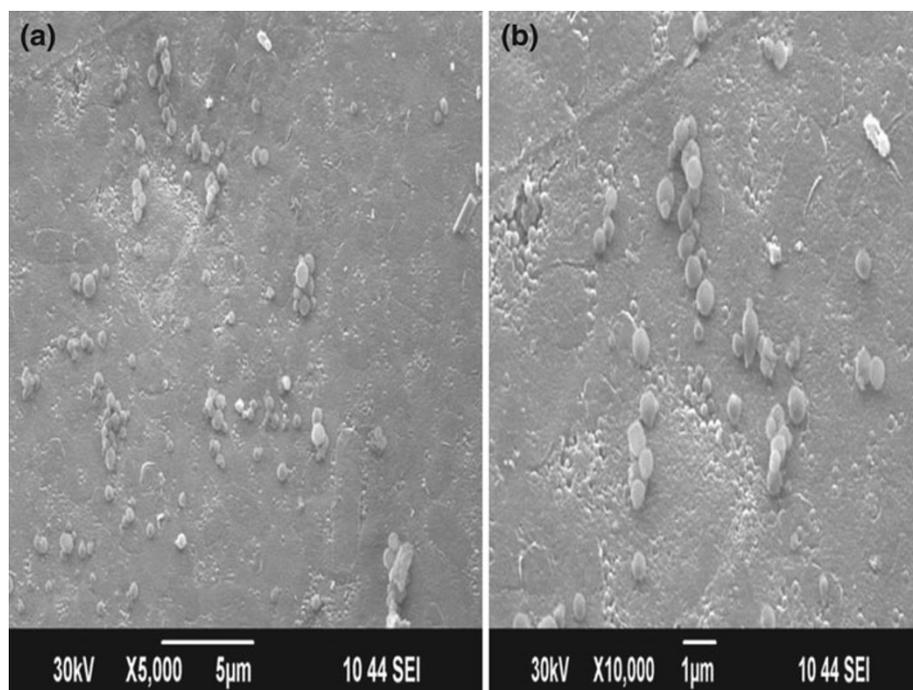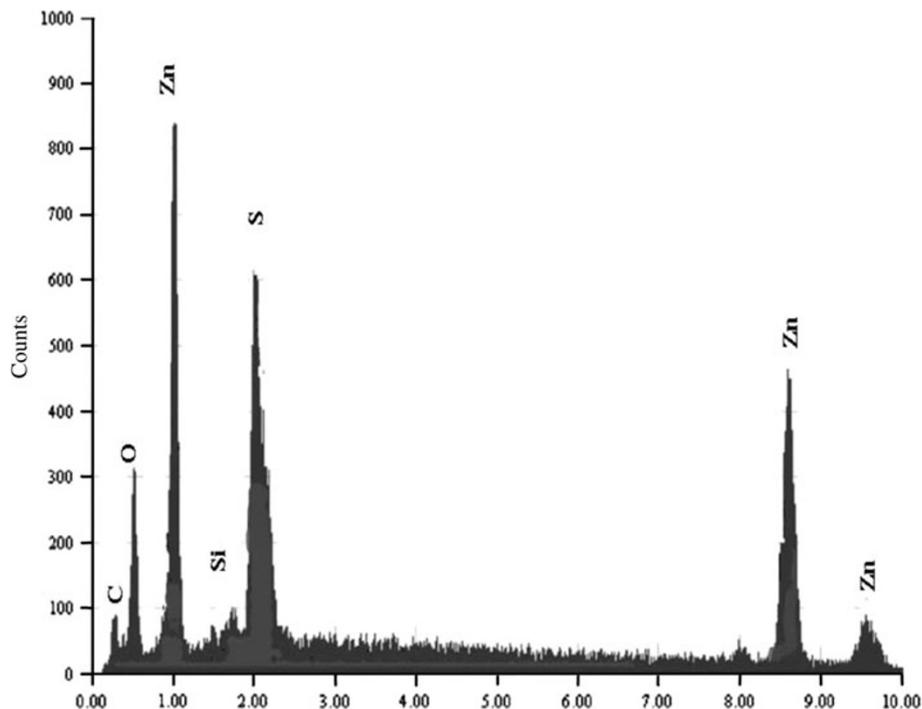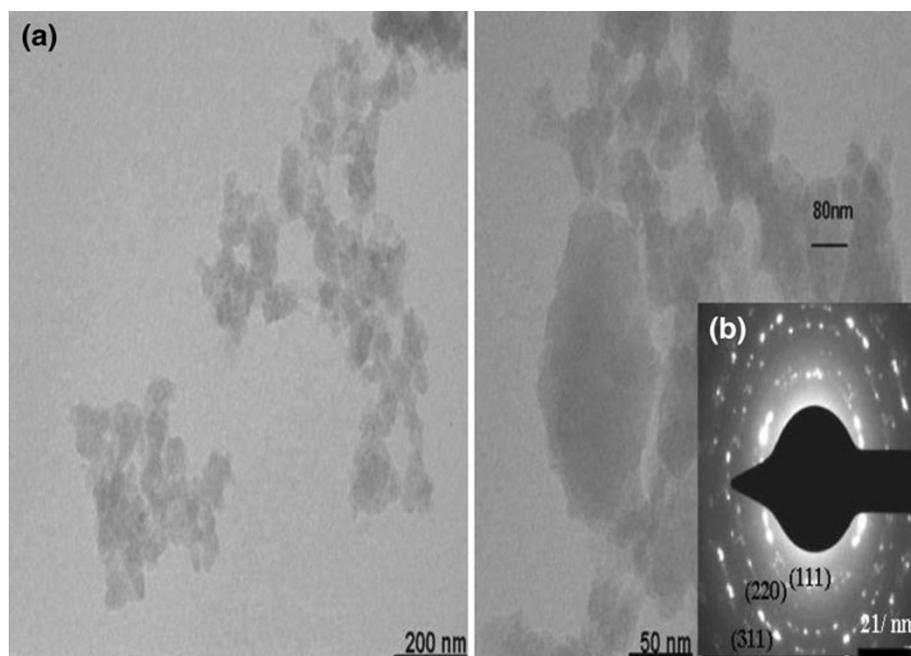
Fig. 4 EDX pattern of zinc

Fig. 5 a and **b** TEM images of nanostructures. The *inset* shows the corresponding SAED pattern of zinc sulfide nanoparticle

halides or bromoalkane vibrations. IR study confirms the presence of amide groups and aliphatic residue proteins have a strong ability to bind to metal, so that the protein is most possibly covered by the metal nanoparticle. It has been earlier reported that protein can bind nanoparticles either through amide or aliphatic groups' residues in the proteins (Basavaraja et al. 2008).

Antimicrobial activity

The antibacterial activity of zinc sulfide nanoparticles against *B. subtilis* and *K. planticola* (purchased from MTCC, Mumbai, India) was studied in Muller Hinton agar. The various concentrations of zinc sulfide nanoparticles were 50 μl, 100 μl and 200 μl. The formation zone was
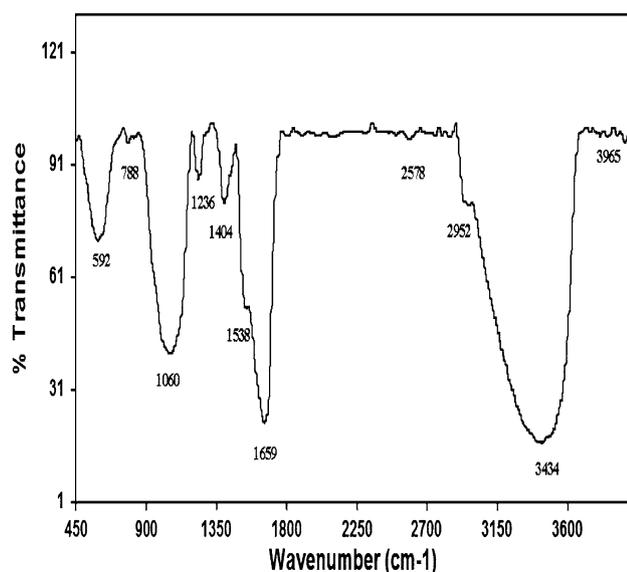
Fig. 6 FTIR spectrum of zinc sulfide nanoparticle synthesized by using *S. nematodiphila*

clearly observed around the disc containing zinc sulfide nanoparticles including clearly moved the antibacterial materials of zinc sulfide nanoparticles. The culture biomass growth rate was compared with and without the addition of zinc sulfide nanoparticles into the disc. The bacterial growth rate of *B. subtilis* (MTCC 3053) and *K. planticola* (MTCC 2277) was decreased on increasing the concentration of zinc sulfide nanoparticles (Table 1). The maximum inhibition zones of zinc sulfide nanoparticles against *B. subtilis* (MTCC 3053) and *K. planticola* (MTCC 2277) were 21.66 ± 0.66 and 22.66 ± 1.454 mm, respectively, with a concentration of 200 μl. The zone of inhibition in the Gram-positive and -negative bacteria can be explained. Gram-negative bacteria showed more inhibition zone than the Gram-positive bacteria due to the cell wall nature of the bacteria. Gram-positive bacteria have thick and chemically complex peptidoglycon in the cell wall, so silver nanoparticles do not easily enter into the cell. But in the Gram-negative bacteria having thin simple multilayered lipid materials in the cell wall, the nanoparticles easily enter into bacterial cells; therefore, these show high inhibition zone than the Gram-positive bacteria (Kim et al. 2007). To the

best of our knowledge, our reports prove that zinc sulfide nanoparticles have more antibacterial activity. The antimicrobial activities of zinc can be used as an effective fungicide in agricultural and food packaging fields (He et al. 2010).

Conclusion

In conclusion, we have successfully synthesized zinc sulfide nanoparticles using *S. nematodiphila* (CAA) which was isolated from a chemical company effluent. The synthesized zinc sulfide nanoparticles exhibited a maximum absorption peak at 390 nm. The morphology of zinc sulfide nanoparticle observed using SEM reveals a spherical shape; elemental analysis of zinc sulfide nanoparticles were characterized using EDX measurements. TEM shows that the particle size was 80 nm with agglomeration. The electron diffraction pattern confirmed the cubic crystalline structure of the zinc sulfide. The FTIR study confirmed that the amide groups of protein could bind with the zinc sulfide nanoparticle. The antibacterial activity of zinc sulfide nanoparticles was studied using different concentrations against *B. subtilis* (MTCC 3053) and *K. planticola* (MTCC 2277) and the maximum inhibition of growth was observed at 200 μl. The inhibitory effects increased on increasing the concentrations of zinc sulfide nanoparticles. The biosynthesis of nanoparticles is used in biomedical and food packaging fields.

Table 1 Growth inhibition of zinc sulfide nanoparticles against *Bacillus subtilis* and *Klebsiella planticola*

Concentration of zinc sulfide nanoparticles	Zone of inhibition (mm in diameter)	
	Bacillus subtilis	*Klebsiella planticola*
50 μl	8.33 ± 0.33	10.66 ± 0.333
100 μl	12.66 ± 1.20	14.00 ± 1.529
200 μl	21.66 ± 0.66	22.66 ± 1.454

± standard deviation

References

Armendariz V, Herrera I, Videa JRP, Yacaman MJ (2004) Size controlled gold nanoparticle. J Nanopart Res 6(4):377–382. doi: 10.1007/s11051-004-0741

Bai HJ, Zhang ZM, Gong J (2006) Biological synthesis of semiconductor zinc sulfide nanoparticles by immobilized *Rhodobacter sphaeroides*. Biotechnol Lett 28:1135–1139. doi:10.1007/s10529-006-9063-1

Baia HJ, Zhang ZM, Guo Y, Yang GE (2009) Biosynthesis of cadmium sulfide nanoparticles by photosynthetic bacteria *Rhodopseudomonas palustris*. Colloids Surf B 70:142–146

Basavaraja S, Balaji SD, Lagashetty A, Rajasab AH, Venkataraman A (2008) A extracellular biosynthesis of silver nanoparticles using the fungus *Fusarium semitectum*. Mater Res Bull 43:1164–1170

Brus LE (1991) Quantum crystallites and nonlinear optics. Appl Phys A 53:465

Elghanian R, Storhoff JJ, Mucic RC, Letsinger RL, Mirkin CA (1997) Selective colorimetric detection of polynucleotides based on the distance-dependent optical properties of gold nanoparticles. Science 277:1078

Giotta L, Agostiano A, Italiano F, Milano F, Trotta M (2006) Heavy metal ion influence on the photosynthetic growth of *Rhodobacter sphaeroides*. Chemosphere 62:1490–1499

Grimont PAD, Jackson TA, Ageron E, Noonan MJ (1988) *Serratia-entomophila* sp. nov. associated with amber disease in the New Zealand grass grub *Costelytra zealandica*. Int J Syst Bacteriol 38:1–6

Håkansson K, Mattiasson B (2002) Microbial degradation of aceto-nitrile using a suspended-carrier biofilm process. Biotechnol Lett 24(4):287–291

He L, Liu Y, Mustapha A, Lin M (2010) Antifungal activity of zinc oxide nanoparticles against *Botrytis cinerea* and *Penicillium expansum*. Microbiol Res 166(3):207–215. doi:10.1016/j.micres.2010.03.003

Hearn WR, Elson MK, Williams RH, Medina-Castro J (1970) Prodigiosin [5-(2-pyrryl-2, 29-dipyrrylmethene] and some substituted prodigiosenes. J Org Chem 35:142–145

Hoffmann MR, Martin ST, Choi WY, Bahnemann DW (1995) Environmental applications of semiconductor photocatalysis. Chem Rev 95:69–96

Joerger R, Klaus T, Granqvist CG (2000) Biologically produced silver–carbon composite materials for optically functional thin film coatings. Adv Mater 12:407–409

Jones HE (1971) Sulfate-reducing bacterium with unusual morphology and pigment content. J Bacteriol 106:339–346

Khan FI, Husain T, Hejazi R (2004) An overview and analysis of site remediation technologies. J Environ Manage 71(2):95–122

Khiewa PS, Radimana S, Huanga NM, Ahmada MS, Nadarajah K (2005) Preparation and characterization of ZnS nanoparticles synthesized from chitosan laurate micellar solution. Mater Lett 59:989–993

Kho R, Torres-Martinez CL, Mehra RK (2000) A simple colloidal synthesis for gram-quantity production of water-soluble ZnS nanocrystal powders. J Colloid Interface Sci 227:561–566. doi:10.1006/jcis.2000.6894

Kim JS, Kuk MSE, Yu KN, Kim JH, Park SJ et al (2007) Antimicrobial effects of silver nanoparticles. Nanomed Nano-technol Biol Med 3:95–101. doi:10.1016/j.nano.2006.12.001

Kowshik M, Deshmukh N, Vogel W, Urban J, Kulkarni SK, Paknikar KM (2002) Microbial synthesis of semiconductor CdS nanoparticles, their characterization, and their use in the fabrication of an ideal diode. Biotechnol Bioeng 78:583–588

Kowshik M, Ashtaputre S, Kharrazi S, Vogel W, Urban J, Kulkarni SK, Paknikar (2003) Extracellular synthesis of silver nanoparticles by a silver-tolerant yeast strain MKY3. Nanotechnology 14:95–101. doi:10.1088/0957/4484/14/1/321

Longoria EC, Nestor ARV, Borja MA (2011) Biosynthesis of silver, gold and bimetallic nanoparticles using the filamentous fungus *Neurospora crassa*. Colloids Surf B 83:42–481

Mandal D, Bolander ME, Mukhopadhyay D, Sarkar G, Mukherjee P (2006) The use of microorganisms for the formation of metal nanoparticles and their application. Appl Microbiol Biotechnol 69:485–492. doi:10.1007/s00253-005-0179-3

Mills A, Hunte L (1997) Overview of semiconductor photo catalysis. J Photochem Photobiol A 108:11–35

Murray CB, Kagan CR, Bawendi MG (1995) Self-organization of CdSe nanocrystallites into 3-dimensional quantum-dot superlat-tices. Science 270:1335–1338

Ngwenya N, Whiteley CG (2006) Recovery of rhodium (III) from solution and industrial wastewaters by a sulphate reducing consortium. Biotechnol Prog 22:1604–1611

Ni Y, Yin G, Hong J, Xua Z (2004) Rapid fabrication and optical properties of zinc sulfide nanocrystallines in a heterogeneous system. Mater Res Bull 39:1967–1972

Penn SG, He L, Natan MJ (2003) Nanoparticles for bioanalysis. Curr Chem Biol 7:609–615

Qiao Z, Xie Y, Qian Y, Zhu Y (2000) γ-Irradiation preparation and characterization of nanocrystalline ZnS. Mater Chem Phys 62:88–90

Rashamuse KJ, Whiteley CG (2007) Bioreduction of Pt (IV) from aqueous solution using sulphate reducing bacteria. Appl Micro-biol Biotechnol 75:1429–1435

Riddin TL, Gericke M, Whiteley CG (2006) Two different hydrog-enase enzymes from sulphate-reducing bacteria are responsible for the bioreductive mechanism of platinum into nanoparticles. Nanotechnology 17:34–82

Sharma NC, Sahi SV, Nath S, Parsons JG, Torresdey JLG, Pal T (2007) Synthesis of plant-mediated gold nanoparticles and catalytic role of biomatrix-embedded nanomaterials. Environ Sci Technol 41(14):5137–5142

Stanley AG (1975) In: Wolfe R (ed) Applied solid state science, vol 15. Academic Press, New York

Subhendu K, Panda DattaA, Chaudhuri S (2007) Nearly monodi-spersed ZnS nanospheres: synthesis and optical properties. Chem Phys Lett 440:235–238

Webb JS, McGinness S, Lappin-Scott HM (1998) Metal removal by sulphate-reducing bacteria from natural and constructed wet-lands. J Appl Microbiol 84(2):240–248

Zhang DB, Qi LM, Cheng HM, Ma JM (2002) Preparation of ZnS nanorods by a liquid crystal template. J Colloid Interface Sci 246:413–416

Zhang CX, Liu JR, Xu MX, Sun J, Yang SY, An X, Gao GF, Lin MS, He ZY, Wu YD, Zhang KY (2008) *Heterorhabditidoides chongmingensis* gen. nov., sp. nov. (Rhabditida: Rhabditidae), a novel member of the entomopathogenic nematodes. J Invertebr Pathol 98:153–168. doi:10.1099/ijs.0.003871-0

Zhang CX, Yang SY, Xu MX, Sun J, Liu H, Liu JR, Liu H, Kan F, Sun J, Lai R, Zhang KY (2009) *Serratia nematodiphila* sp. nov., associated symbiotically with the entomopathogenic nematode *Heterorhabditidoides chongmingensis* (Rhabditida: Rhabditi-dae). Int J Syst Evol Microbiol 59:1603–1608

Zhao Z, Geng F, Cong H, Bai J, Cheng HM (2006) A simple solution route to controlled synthesis of ZnS submicrospheres, nanosheets and nanorods. Nanotechnology 17:4731–4735